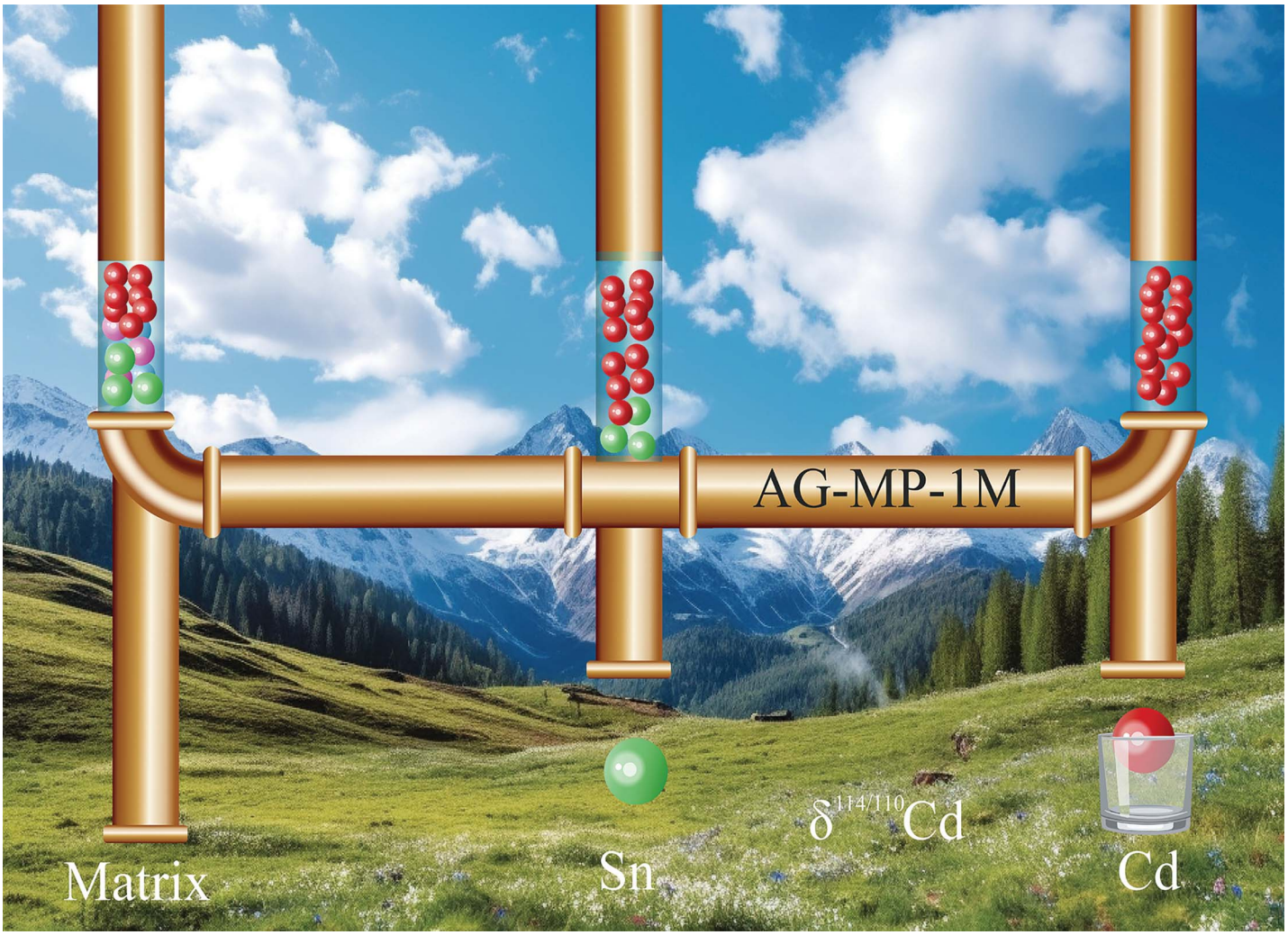

Showcasing research from Professor Jie Li's laboratory, Guangzhou Institute of Geochemistry, Chinese Academy of Sciences, Guangzhou, 510640, China.

A single-stage anion exchange separation method for Cd isotopic analysis in geological and environmental samples by MC-ICP-MS

This paper demonstrates a single-stage purification procedure for Cd with AG-MP-1M anion exchange resin and measurements of Cd isotopes by MC-ICP-MS. The method takes advantage of the different affinity of Sn and Cd on AG-MP-1M resin in different concentrations of HCl and HF in mixed HCl-HF solutions. The interference of Sn can be removed from the resin using 2 M HCl-4 M HF solution, and Cd fraction is eluted by 0.005 M HCl-2 M HF solution while potential residual Sn can be retained on the resin.

As featured in:

See Jie Li *et al.*,
J. Anal. At. Spectrom., 2023, **38**, 2291.

ROYAL SOCIETY OF CHEMISTRY

rsc.li/jaas

Registered charity number: 207890

JAAS

ROYAL SOCIETY OF CHEMISTRY

PAPER

View Article Online
View Journal | View Issue

Cite this: *J. Anal. At. Spectrom.*, 2023, **38**, 2291

A single-stage anion exchange separation method for Cd isotopic analysis in geological and environmental samples by MC-ICP-MS†

Qiao-Hui Zhong,[abc] Lu Yin,[d] Jie Li, *[ab] Yue-Xing Feng, [eg] Neng-Ping Shen,[f] Bing-Yu Peng[abc] and Zhao-Yang Wang[abc]

AG-MP-1M anion exchange resin is commonly used to separate and purify Cd from geological and environmental samples. However, a second column using anion exchange, TRU Spec, or BPHA extraction resins is also required to further purify Cd from the residual Sn for high-precision Cd isotope ratio measurements. In this study, a new and efficient single-stage separation method using AG-MP-1M (100–200 mesh) anion exchange resin was developed to separate Cd from geological and environmental samples for high-precision Cd isotope ratio measurements. Most of the Sn (>99%) is effectively stripped from the resin using a 2 M HCl + 4 M HF mixed eluent, unlike commonly used separation protocols with AG-MP-1M anion exchange resin, which only removes ~65% of the Sn using HCl eluent. Furthermore, potential residual Sn is retained on the resin by elution of 0.04 M HCl + 2 M HF and 0.005 M HCl + 2 M HF, which allows quantitative collection of the Cd fraction (~99.5%) without Sn tailing. The single-stage purification procedure takes advantage of the different affinities of Sn on AG-MP-1M anion exchange resin at different HCl and HF concentrations in mixed HCl + HF solutions, which allows direct and effective separation of Cd from Sn and other complex sample matrices. We used this procedure and the double-spike MC-ICP-MS method to determine the $\delta^{114/110}Cd_{NIST\ SRM\ 3108}$ values for Mn nodule, igneous rock, shale, soil, and sediment reference materials, and obtained results that agree within analytical uncertainty with the values reported in previous studies. In addition, the $\delta^{114/110}Cd_{NIST\ SRM\ 3108}$ values of soil (GSS-1a), sediment (GSD-4a), and dolomite (GSR-12) standard reference materials are reported for the first time in this paper. The described purification procedure allows efficient and rapid Cd isotopic analysis in different types of geological and environmental samples.

Received 16th July 2023
Accepted 19th September 2023

DOI: 10.1039/d3ja00234a

rsc.li/jaas

1. Introduction

Cadmium is a chalcophile, toxic, and moderately volatile element with a main valence state of +2 and eight stable isotopes: ^{106}Cd (1.25%), ^{108}Cd (0.89%), ^{110}Cd (12.47%), ^{111}Cd (12.80%), ^{112}Cd (24.11%), ^{113}Cd (12.23%), ^{114}Cd (28.75%), and ^{116}Cd (7.51%).[1–3] In the past two decades, mass-dependent Cd isotopic variations have been investigated in different geological and environmental samples, which exhibit isotopic fractionation related to numerous (bio)geochemical and environmental processes, such as biological uptake,[4–6] adsorption/co-precipitation,[7–12] weathering,[13–15] and evaporation/condensation processes.[16–20] The potential for Cd isotopes to track low-temperature geological and environmental processes on the Earth's surface and cosmochemical processes has been reported in various studies.[21–38] These studies have shown that Cd isotopes are a promising tool for geological and environmental applications.

Cadmium isotope data were initially determined by thermal ionisation mass spectrometry (TIMS) combined with the double-spike method for instrumental mass bias correction, but had large analytical uncertainties of ±0.24‰ to ±4‰ (2SD).[39,40] With further developments in mass spectrometry, high-precision methods for Cd isotopic analysis by multi-collector-inductively coupled plasma-mass spectrometry (MC-ICP-MS) and TIMS have been widely reported, and the long-term analytical precision can be better than ±0.1‰ (2SD).[41–51]

[a]State Key Laboratory of Isotope Geochemistry, Guangzhou Institute of Geochemistry, Chinese Academy of Sciences, Guangzhou, 510640, China. E-mail: jieli@gig.ac.cn
[b]CAS Center for Excellence in Deep Earth Science, Guangzhou, 510640, China
[c]College of Earth and Planetary Sciences, University of Chinese Academy of Sciences, Beijing, 100101, China
[d]Hebei Key Laboratory of Strategic Critical Mineral Resources, Hebei GEO University, Shijiazhuang, 050031, China
[e]Southern Marine Science and Engineering Guangdong Laboratory (Zhuhai), Zhuhai, 519082, PR China
[f]State Key Laboratory of Ore Deposit Geochemistry, Institute of Geochemistry, Chinese Academy of Sciences, Guiyang, 550081, China
[g]Radiogenic Isotope Facility, School of Environment, The University of Queensland, Brisbane, QLD 4072, Australia

† Electronic supplementary information (ESI) available. See DOI: https://doi.org/10.1039/d3ja00234a

Table 1 Isobars and molecular interfering ions for Cd isotopic measurements[a]

Mass/abundance	Molecular interference	Isobar interference
^{106}Cd (1.25%)	$^{66}Zn^{40}Ar^+$, $^{90}Zr^{16}O^+$	
^{108}Cd (0.89%)	$^{68}Zn^{40}Ar^+$, $^{92}Zr^{16}O^+$, $^{92}Mo^{16}O^+$	^{108}Pd (26.46%)
^{110}Cd (12.5%)	$^{70}Zn^{40}Ar^+$, $^{70}Ge^{40}Ar^+$, $^{94}Zr^{16}O^+$, $^{94}Mo^{16}O^+$, $^{92}Mo^{18}O^+$, $^{109}Ag^1H^+$, $^{93}Nb^{17}O^+$	^{110}Pd (11.72%)
^{111}Cd (12.8%)	$^{71}Ga^{40}Ar^+$, $^{95}Mo^{16}O^+$, $^{97}Mo^{14}N^+$, $^{93}Nb^{18}O^+$	
^{112}Cd (24.1%)	$^{72}Ge^{40}Ar^+$, $^{96}Zr^{16}O^+$, $^{96}Mo^{16}O^+$, $^{96}Ru^{16}O^+$, $^{98}Mo^{14}N^+$, $^{76}Se^{36}Ar^+$	^{112}Sn (0.973%)
^{113}Cd (12.2%)	$^{73}Ge^{40}Ar^+$, $^{97}Mo^{16}O^+$, $^{99}Ru^{14}N^+$, $^{77}Se^{36}Ar^+$	^{113}In (4.288%)
^{114}Cd (28.7%)	$^{74}Ge^{40}Ar^+$, $^{98}Mo^{16}O^+$, $^{98}Ru^{16}O^+$, $^{100}Ru^{14}N^+$, $^{100}Mo^{14}N^+$, $^{77}Se^{36}Ar^+$, $^{74}Se^{40}Ar^+$	^{114}Sn (0.659%)
^{116}Cd (7.49%)	$^{76}Ge^{40}Ar^+$, $^{100}Mo^{16}O^+$, $^{100}Ru^{16}O^+$, $^{76}Se^{40}Ar^+$, $^{80}Se^{36}Ar^+$	^{116}Sn (14.536%)

[a] From the literature of Wombacher *et al.* (2003)[2]

Lu *et al.* (2023)[52] proposed a double spike-standard addition technique by adding a certified standard solution containing a Cd double-spike with a known isotopic composition to a sample to increase the amount of Cd. This method is required with lower sample consumption and is beneficial for the Cd isotopic measurement of ultra-trace amounts of Cd in samples.[51] However, this method requires complex calculations after the measurements. Irrespective of the measurement method, Cd isotopic measurements by mass spectrometry are sensitive to the residual matrix in the purified samples, which may cause matrix effects, and polyatomic and isobaric interferences (Table 1). Therefore, due to the complex matrix and relatively low Cd concentrations in geological and environmental samples, establishing an efficient Cd purification procedure is required for high-precision Cd isotopic measurements.

AG1-X8 anion exchange resin is generally utilised to purify Cd from various natural materials. For examples, two-step anion exchange column chromatography utilising AG1-X8 anion exchange resin (200–400 mesh) has been successfully used for Cd separation, in which two anion exchange columns are utilised to remove most of the matrix elements, and then to separate Cd from Sn, respectively.[42,53,54] In addition, a two-stage column chemistry with AG1-X8 anion exchange resin (100–200 mesh) and TRU Spec resin has been widely utilised for Cd separation from geological samples, whereby an anion exchange column is used to remove most matrix elements, which is followed by a TRU Spec resin column to further separate Cd from Sn.[2,6,18,19,43,55] However, TRU Spec resin-derived organic compounds can be introduced into the purified Cd solutions and lead to erroneous isotopic results even with a double-spike correction, which is due to phosphor bound organics.[56,57] Zhong *et al.* (2023)[50] investigated the interference of P on Cd isotopic measurements, and showed this is mainly caused by P-related matrix effects, which further confirmed the interference of a TRU Spec resin-derived P-related matrix on Cd isotopic measurement. To remove TRU Spec resin-derived P organic compounds, Murphy *et al.* (2016)[57] used liquid–liquid extraction with *n*-heptane. Liu *et al.* (2019)[46] reported a single-stage AG1-X8 anion exchange resin (100–200 mesh) separation method for Cd isotope analysis of various geological samples by MC-ICP-MS. Although all these purification procedures have been successfully used for Cd isotopic analysis, relatively large volumes of eluent and numerous evaporation/transfer steps are required, which increases the column separation time and potential blank levels.

In addition to AG1-X8 anion exchange resin, AG-MP-1M anion exchange resin has been widely used to separate Cd from various types of samples. However, Cd cannot be quantitatively separated from Sn with a single-stage AG-MP-1M (100–200 mesh) column.[44,45,47,49,50,58,59] Therefore, two-step AG-MP-1M anion exchange resin (100–200 mesh) column chromatography has been successfully used for Cd separation from geological and environmental samples, whereby the two anion exchange columns are utilised to first remove most of the matrix elements and then mainly to purify Cd from the residual Sn.[47] In addition, two-step column chromatography using AG-MP-1M anion exchange resin (100–200 mesh) and TRU Spec resin has been successfully used for Cd separation from environmental samples, whereby an anion exchange column is used to remove most matrix elements, and the TRU Spec resin column is used to further purify Cd from the residual Sn.[49] Zhong *et al.* (2023)[50] also reported a two-step chromatographic method for Cd separation from geological samples. Considering the risk of P-related interferences from TRU Spec resin, BPHA extraction resin was used instead of TRU Spec resin to further purify Cd from residual Sn after separation of Cd using an AG-MP-1M anion exchange resin column. These two-step chromatography methods can achieve good Cd separation, but require relatively large volumes of eluent and numerous evaporation/transfer steps, which increases the column separation time, elution steps, and potential blank levels.

In this study, we describe a new single-stage separation procedure with the anion exchange resin AG-MP-1M (100–200 mesh) for separating and purifying Cd from geological and environmental samples. We used this procedure and the double-spike MC-ICP-MS method to determine the Cd isotope ratios in geological and environmental reference materials. Repeated measurements of these reference materials yielded $\delta^{114/110}Cd_{NIST\ SRM\ 3108}$ values in good agreement with their recommended values.

2. Experimental procedures

2.1. Reagents and samples

Mineral acids of BVIII grade reagents (Beijing Institute of Chemical Reagents, China) were purified twice (HF, HCl, and HNO_3) in a Savillex DST-1000 sub-boiling acid distillation

system (Savillex, Eden Prairie, Minnesota, USA). Ultra-pure water (Milli-Q H_2O; 18.2 MΩ cm) from a Millipore purification system was utilised for mixing the reagents. The standard solution NIST SRM 3108 was used as the Cd isotopic standard material, and Spex Cd was used as a laboratory reference material. NIST SRM 3108 was purchased from the National Institute of Standards and Technology (NIST), USA. Spex Cd was generously provided by Dr Zhu at the China University of Geosciences, Beijing, China. ICP-MS standard solutions (1000 μg mL^{-1}) of Cd and Sn were purchased from the Beijing General Research Institute for Nonferrous Metals (BGRINM), China. In addition, we analysed and report the Cd isotopic compositions of 12 geological and environmental reference materials, including 3 rocks (BHVO-2, GSP-2, and COQ-1), 1 shale (SGR-1b), 1 soil (NIST 2711a), and 2 Mn nodules (NOD-P-1 and -A-1) from the United States Geological Survey; and 3 stream sediments (GSD-3a, -4a, and -5a), 1 dolomite (GSR-12), and 1 soil (GSS-1a) from the Institute of Geophysical and Geochemical Prospecting, People's Republic of China.

2.2. Sample digestion

For the rocks, shale, sediments, and soil reference materials, 25–400 mg of sample powders containing 30–100 ng Cd (typically 30 ng) were accurately weighed into Teflon bombs. Cadmium spike solutions were accurately weighed into the Teflon sample bombs to achieve $Cd_{spike} : Cd_{sample} = 1 : 1$, and to avoid Cd isotopic fractionation during sample dissolution and chemical purification. Subsequently, 1 mL of concentrated HNO_3 (15.3 mol L^{-1}) and 2.0 mL of HF (22 mol L^{-1}) were added to the Teflon bombs, which were then sealed and placed in an oven at 190 °C for 72 h to breakdown and dissolve the solid minerals and organic materials. The samples were then transferred to Savillex™ PFA beakers and evaporated to dryness. To completely dissolve the samples, *aqua regia* ($HCl : HNO_3 = 3 : 1$; v/v) was added to the Savillex™ PFA beakers, which were left on a hotplate at 130 °C overnight. Subsequently, 4 mL of 6 M HCl was added to the Savillex™ PFA beakers to completely decompose the residues. For the Mn nodules and carbonate rocks, 25–360 mg of each sample powder containing 30–100 ng Cd (typically 30 ng) was accurately weighed into Savillex™ PFA beakers. After the Cd spike solutions were accurately weighed and added to the PFA beakers, 4 mL of 6 M HCl was slowly added to the samples, which were capped tightly and then heated at 120 °C overnight. After evaporating the samples, 3 mL of 6 M HCl was added to the Savillex™ PFA beakers to decompose the residual solids and convert these to chlorides. Finally, after evaporating the samples, the sample solutions were redissolved in 2–3 mL of 2 M HCl for chemical separation.

2.3. Cadmium purification

Chemical separations were conducted in a class 100 clean hood at the State Key Laboratory of Isotope Geochemistry, Guangzhou Institute of Geochemistry, Chinese Academy of Sciences (GIG-CAS), Guangzhou, China. The column protocol is outlined in Table 2 and described briefly here. A volume of 1.9 mL of AG-MP-1M anion exchange resin was packed in a Teflon column (15 cm × 6 mm i.d.), which was washed with 2 M HNO_3 and MilliQ-H_2O, respectively, and then conditioned with 2 M HCl. After an aliquot of the spiked sample solution (2–3 mL) was loaded onto the column, another 8 mL of 2 M HCl were added to elute matrix elements (*e.g.*, Na, Mg, Fe, Mn, Zr, Cu, Ni, Pb, Ge, REE, and Cr). Subsequently, Sn, Pb, In and Mo were removed using 2 M HCl + 4 M HF, and Zn together with little Nb/In was eluted by using 16 mL of 0.05 M HCl. 10 mL eluent of 0.04 M HCl + 2 M HF can further remove the potential residual matrix, but retain potential Sn on the resin. Finally, the Cd fraction was collected in 0.005 M HCl + 2 M HF and then evaporated to dryness. The samples were then dissolved in 0.03 mL of concentrated HNO_3 and evaporated (this procedure was performed twice). Subsequently, 2% (v/v) HNO_3 was used to redissolve the samples, prior to analysis with a Neptune Plus MC-ICP-MS.

2.4. Mass spectrometry

Cadmium isotopic compositions were measured with a Neptune Plus MC-ICP-MS at the Hebei Key Laboratory of Strategic Critical Mineral Resources, Hebei GEO University, Shijiazhuang, China. The Neptune Plus is equipped with nine Faraday cups connected to 10^{11} Ω amplifiers and eight ion counters, which can measure isotope ratios over a relative mass range of up to 17%. Cadmium isotopic measurements were conducted in static mode at low mass resolution (~400), and the data were collected for 1 block with 40 measurement cycles with an integration time of 4.194 s per cycle. The samples were introduced into the plasma with an Aridus III desolvator (Teledyne CETAC Technologies, Omaha, USA) equipped with a 100 mL min^{-1} PFA nebuliser system. The typical signal intensity (^{110}Cd) was 1.3–1.7 V for a 10 ng mL^{-1} Cd

Table 2 Elution sequence of the single-stage column procedure

Column procedure	Eluant	Volume (mL)
AG-MP-1M (100–200 mesh)		1.9
Cleaning	2 M HNO_3	10
Cleaning	MilliQ-H_2O	3
Condition	2 M HCl	10
Loading	2 M HCl	2–3
Matrix removal (Mg, Ca, Nb, Fe, Ga, Ge, Ag, Zr, *etc.*)	2 M HCl	8
Matrix removal (Sn, Mo, and In)	2 M HCl + 4 M HF	16
Matrix removal (Zn)	0.05 M HCl	16
Matrix removal (residual)	0.04 M HCl + 2 M HF	10
Collecting Cd	0.005 M HCl + 2 M HF	14

Table 3 Typical instrumental setup during Neptune Plus MC-ICP-MS analysis

Rf power	1223 W						
Auxiliary gas (Ar) flow rate	0.89 L min^{-1}						
Sample gas (Ar) flow rate	1.094 L min^{-1}						
Cooling gas (Ar) flow rate	15.50 L min^{-1}						
Measurement mode	Static						
Interface cones	H sample cone + X skimmer cone (nickel)						
Acceleration voltage	10 kV						
Detection system	Faraday cups						
Amplifier	10^{11} Ω						
Idle time	3.000 s						
Integration time	4.194 s						
Mass resolution	~400 (low)						
Spray chamber	Dual cyclonic-Scott (quartz)						
Cd sensitivity	360–400 V ppm^{-1} (low-resolution)						
Sample uptake	100 μL min^{-1}						
Desolvation nebulizer	Aridus III						
Sweep gas flow rate	2.75 L min^{-1}						
Nitrogen gas	2.6 L min^{-1}						
Desolvation temperature	140 °C						
Spray chamber temperature	104 °C						
Cup configuration	L3	L2	L1	C	H1	H3	H4
	^{110}Cd	^{111}Cd	^{112}Cd	^{113}Cd	^{114}Cd	^{116}Cd	^{119}Sn

solution, corresponding to an instrumental sensitivity of 1040–1361 V ppm^{-1}. The inlet system of the instrument was cleaned with 3% (v/v) HNO_3 + 0.1% HF and 3% (v/v) HNO_3 solutions between each measurement, until the ^{110}Cd signal decreased to <2 mV after ~5 min. The typical instrumental operating parameters are summarised in Table 3. All the measured raw data were subjected to a double-spike correction procedure that used an in-house Microsoft Virtual Basic program based on a mathematical algorithm.[60] Cadmium isotope ratios are reported in delta (δ) notation as the per mil (‰) deviation relative to NIST SRM 3108, as follows:

$$\delta^{114/110}Cd_{\text{NIST SRM 3108}} = ([^{114}Cd/^{110}Cd]_{\text{sample}}/[^{114}Cd/^{110}Cd]_{\text{NIST SRM 3108}} - 1) \times 1000.$$

2.5. Elemental analysis

During the Cd separation, elemental mass fractions were determined for all the collected aliquots with an ICP-MS (Thermo-Scientific X Series-2) at the State Key Laboratory of Isotope Geochemistry, GIG-CAS. For the drift corrections during ICP-MS analysis, Rh and Re as internal standards were added to all samples and a quality control solution (*i.e.*, the drift monitor). The latter was analysed repeatedly during the ICP-MS measurements. The relative standard deviations (RSDs) of elements measured by ICP-MS were less than ±5%.

3. Results and discussion

3.1. Optimisation of the Cd separation procedures

Previous studies have shown that in a HCl medium, most Sn is still retained on the AG-MP-1M anion exchange resin during Cd elution, which results in different levels of Sn in the Cd solution for samples with complex matrices.[47,50,58] A mixture of HF and HCl may be an alternative way to separate Cd from Sn on AG-MP-1M anion exchange resin.[61,62] To validate this approach, a basalt standard (BHVO-2; doped with different Cd and Sn single standard solutions to a Sn/Cd ratio of ~4) was utilised in our separation experiments.

The samples dissolved in 1.2 M HCl,[58] and 2 M HCl[44,47,49,50,59] have been used as the loading medium during Cd separation on AG-MP-1M anion exchange resin. In this study, samples dissolved in 1 M and 2 M HCl were used for loading. As shown in Fig. 1a, the sample solution in 2 mL of 1 M HCl was added to the column and sequentially washed with 1 M HCl, which can quickly remove most matrix elements (*e.g.*, Ca, K, Mg, Fe, Ni, Ga, Ge, Zr, Mo, Pd, Ag, and Pb) but causes breakthrough of ~1.5% Cd (Fig. S1a†). Similarly, the matrix (Ca, K, Mg, Fe, Ni, Ga, Ge, Zr, Mo, Pd, Ag, and Pb) can be removed from the 2 mL of loading solution together with subsequent elution of 2 M HCl, and Cd is retained on the resin (Fig. 1b and c; S1b and c†).

Previous studies have shown that <70% of the Sn fraction is slowly eluted and severely tails from the eluted 0.06 M HCl to the eluted 0.0012 M HCl for Cd collection.[47,50,58] In a HCl medium, Cd and Sn have similar adsorption capacities on AG-MP-1M anion exchange resin, which results in incomplete separation between Cd and Sn.[50] However, mixed solutions of HF + HCl can considerably change the adsorption capacities of Sn on anion exchange resin.[61,62] In the present study, 0.2 M HCl + 4 M HF, 1 M HCl + 4 M HF, and 2 M HCl + 4 M HF solutions were used to evaluate their capacity to strip Sn from the anion exchange resin. Almost all the Sn can be eluted with 2 M HCl + 4 M HF, and most of the Sn is removed with 1 M HCl + 4 M HF, although there is slight Sn tailing, whereas only ~5% of the Sn can be eluted with 0.2 M HCl + 4 M HF (Fig. 1). These results show that the adsorption capacities of Sn on AG-MP-1M anion exchange resin decrease gradually from 0.2 M HCl + 4 M HF to 2 M HCl + 4 M HF (Fig. 1a–c). In addition, we found that Sn can be eluted from AG-MP-1M anion exchange resin with 2 M HF, although Cd is also stripped from the resin (the separation curve is not shown here). Therefore, both the HF and HCl in the mixed HCl + HF solution control the adsorption capacities of Sn on AG-MP-1M anion exchange resin.

Surprisingly, ~76.3% Cd (Fig. S1a†) along with the Zn fraction can be eluted with 0.025 M HCl after the elution of 1 M HCl + 4 M HF (Fig. 1a). The Cd fraction was not stripped and the Zn fraction and residual matrix elements were removed by using 0.05 M and 0.015 M HCl, respectively, after the elution of 2 M HCl + 4 M HF (Fig. 1b and S1b†). Interestingly, no Sn was removed by either 0.05 M HCl + 2 M HF or 0.015 M HCl + 2 M HF, after the elution of 0.2 M HCl + 4 M HF (Fig. 1c), which may be due to the high adsorption capacity of Sn on AG-MP-1M anion exchange resin in both 0.05 M HCl + 2 M HF and 0.015 M HCl + 2 M HF. In previous studies, 0.0012 M HCl has always been utilised to collect Cd from the AG-MP-1M anion exchange resin column.[47,50,58] In the present study, 0.0012 M HCl (the separation curve is not shown here) and Milli-Q H_2O were used to collect Cd (~92.7%, Fig. S1b†), but trace amounts of Sn remained in the Cd cut (Fig. 1b). In addition, the Cd fraction

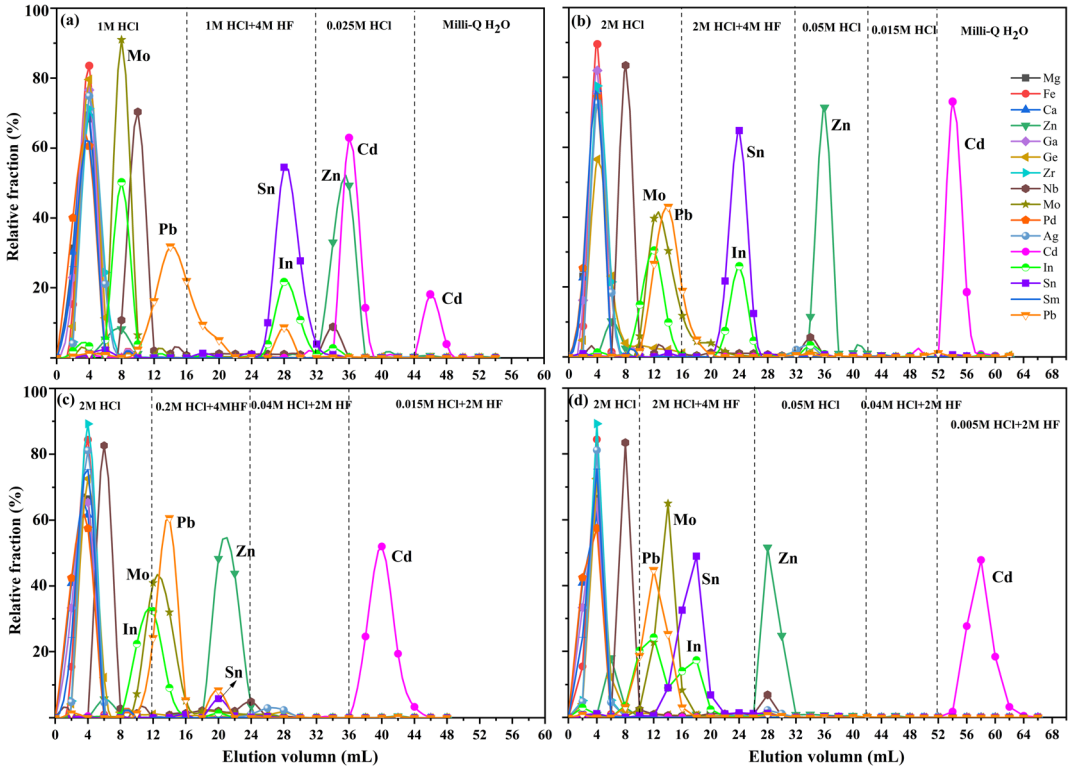

Fig. 1 Elution curves of the Cd purification procedures using different reagents on AG-MP-1M anion exchange (100–200 mesh) resin. (a), (b) and (c) represent the elution curves of trace elements and Cd with AG-MP-1M resin. Different molarities of HCl (1, 2, 0.05 and 0.025 M) and the molarities of mixed acid (HCl + HF) were tested; (d) represents the elution curve of trace elements and Cd using AG-MP-1M anion exchange (100–200 mesh) resin.

(~99.1%, Fig. S1c†) can be collected earlier using 0.015 M HCl + 2 M HF without Sn tailing (Fig. 1c).

Based on these results, the purification procedures shown in Fig. 1b and c can potentially be utilised to separate and purify Cd from the matrix of natural samples. Four BHVO-2 samples (with a Sn standard solution added to ~0.1 g BHVO-2) with different Sn/Cd ratios (*e.g.*, 10, 50, 200, and 500) were purified using the purification procedures shown in Fig. 1b and c. However, the four samples subjected to the purification procedure in Fig. 1b contain residual Sn, which increases as the initial Sn/Cd ratios of the samples increase. This demonstrates that Sn cannot be completely removed by using 2 M HCl + 4 M HF, and the residual Sn fraction may be eluted into the Cd cut for samples with high Sn/Cd ratios. Furthermore, apart from the sample with Sn/Cd = 10, the other samples with higher Sn/Cd ratios subjected to the purification procedure in Fig. 1c also contain residual Sn in the Cd cuts. It is clear that when samples have a high Sn/Cd ratio (*e.g.*, >10 to 500), Sn cannot be strongly adsorbed on the resin, and some Sn will be collected in the Cd cut during Cd elution.

Our experiments show that the adsorption capacity of Sn on AG-MP-1M anion exchange resin increases gradually with decreasing HCl concentrations in the mixed HCl + HF (*e.g.*, from 2 M HCl + 4 M HF to 0.015 M HCl + 2 M HF), which indicates that both HCl and HF in the mixture control the distribution coefficient of Sn on AG-MP-1M anion exchange resin (Fig. 1). This may be due to the complexes formed between Sn^{4+}, and Cl^- and F^- ions. In 2 M HCl + 4 M HF or 1 M HCl + 4 M HF, the Sn^{4+}, Cl^-, and F^- may occur mainly as Sn chloride/fluoride complex ions such as $SnF_2Cl_4^{2-}$ and $SnF_3Cl_3^{2-}$, which have a low adsorption capacity on AG-MP-1M anion exchange resin. Moreover, Sn can also be eluted from AG-MP-1M anion exchange resin with 2 M HF, possibly to form SnF_6^{2-}, which has a low distribution coefficient on the resin, unlike Sn chloride/fluoride complex ions in a mixed acid solution with a low HCl concentration (*e.g.*, 0.2 M HCl + 4 M HF to 0.015 M HCl + 2 M HF).

Based on these experiments, we optimised the column separation procedure (Table 2; Fig. 1d and S1d†). Following sample loading and removal of most of the matrix with 2 M HCl, most of the Sn is effectively removed by elution of 2 M HCl + 4 M HF. The Zn fraction and residual matrix are subsequently removed with 0.05 M HCl and 0.04 M HCl + 2 M HF. Compared with 0.015 M HCl + 2 M HF, 0.005 M HCl + 2 M HF can more quickly elute Cd without Sn tailing. Therefore, the quantitative collection of the Cd fraction (~99.5%, Fig. S1d†) is undertaken with 0.005 M HCl + 2 M HF, and potential residual Sn is strongly retained on the resin by elution of 0.04 M HCl + 2 M HF and 0.005 M HCl + 2 M HF. This procedure takes advantage of the different affinities of Sn for AG-MP-1M anion exchange resin

with different concentrations of HCl and HF in a mixed HCl + HF solution. As such, this technique can effectively separate pure Cd from the matrix element, and eliminate Sn in the Cd cut, which allows high-precision and accurate determination of Cd isotope ratios.

3.2. Evaluation of matrix effects, and molecular and isobaric interferences

Some elements can generate direct isobars interferences and potentially form argide-, nitride-, and oxide-related molecular interferences during Cd isotope analysis (Table 1). To assess the effectiveness of our purification method, the Cd cuts from six reference materials (GSP-2, BHVO-2, NOD-P-1, COQ-1, GSD-5a, and GSS-1a) purified by the presented procedure (Table 1) were analysed by ICP-MS.

The results show that the matrix elements are efficiently removed from Cd with the residual element/Cd ratios being <0.02% (Fig. 2). For example, matrix elements such as Mg, P, Ca, Fe, Sm, and Pb have matrix element/Cd ratios of <0.0002, which are much lower than those that can cause matrix effects as constrained by doping experiments.[46,47,50,55,56,58] For the elements that form molecular interferences on Cd isotopes, the Zn/Cd, Ga/Cd, Ge/Cd, Zr/Cd, Nb/Cd, Mo/Cd, and Ag/Cd ratios in the six Cd cuts are lower than 0.000121, 0.000013, 0.000088, 0.000110, 0.000130, 0.000100, and 0.000134, respectively (Fig. 2). Furthermore, Sn, In, and Pd have direct isobaric interferences on Cd isotopes, and the Cd cuts have Sn/Cd, In/Cd, and Pd/Cd ratios that are lower than 0.000125, 0.000012, and 0.000004, respectively (Fig. 2). The results indicate that matrix elements are effectively separated from Cd and reduced to very low levels in the Cd cut (Fig. 3), which are lower than those that can cause matrix effects or molecular and isobaric interferences during Cd isotope analysis.[44,46,47,49,56,59] As such, the presented analytical protocols (Table 2) are suitable for purifying Cd and the high-precision and accurate determination of Cd isotope ratios.

3.3. Precision and accuracy of the Cd isotopic analysis

We assessed the precision and accuracy of our Cd isotopic analysis. Cadmium standard solutions NIST SRM 3108 and Spex-Cd were measured repeatedly to evaluate the instrumental stability. Repeated analysis of NIST SRM 3018 over 18 months yielded an average $\delta^{114/110}Cd_{NIST\ SRM\ 3018}$ value of $-0.001 \pm 0.043‰$ (2SD; $n = 500$) (Fig. 3a). Spex Cd was used as a secondary standard to monitor the stability during sample analysis. The long-term measurements of Spex Cd yielded a $\delta^{114/110}Cd_{NIST\ SRM\ 3018}$ value of $-2.103 \pm 0.056‰$ (2SD; $n = 52$) (Fig. 3b), which is in agreement with the values of $-2.13 \pm 0.09‰$ (2SD; $n = 74$), $-2.121 \pm 0.042‰$ (2SD; $n = 18$), and $-2.094 \pm 0.049‰$ (2SD; $n = 16$) reported by Li *et al.* (2018),[59] Tan *et al.* (2020),[47] and Zhong *et al.* (2023),[50] respectively.

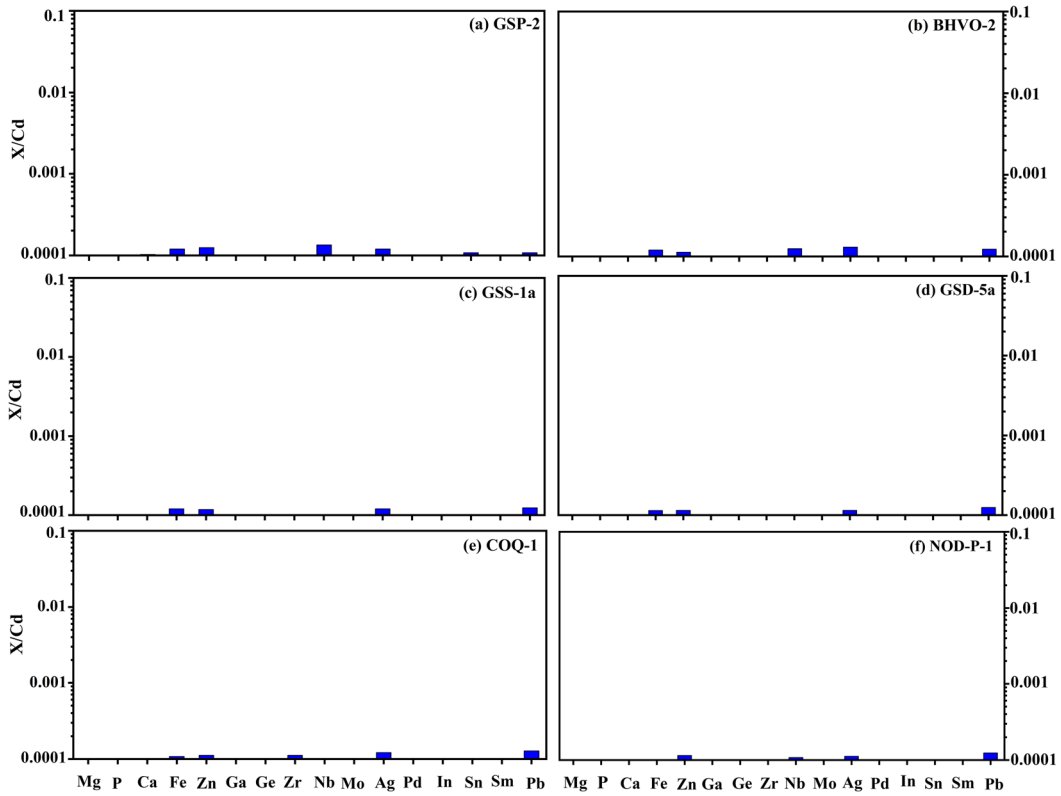

Fig. 2 Purification effectiveness of protocols at removing matrix elements for six selected samples:(a) GSP-2, (b) BHVO-2, (c) GSS-1a, (d) GSD-5a, (e) COQ-1, and (f) NOD-P-1. The concentration ratio of the matrix element to Cd is expressed as [X]/[Cd] (where X denotes a matrix element).

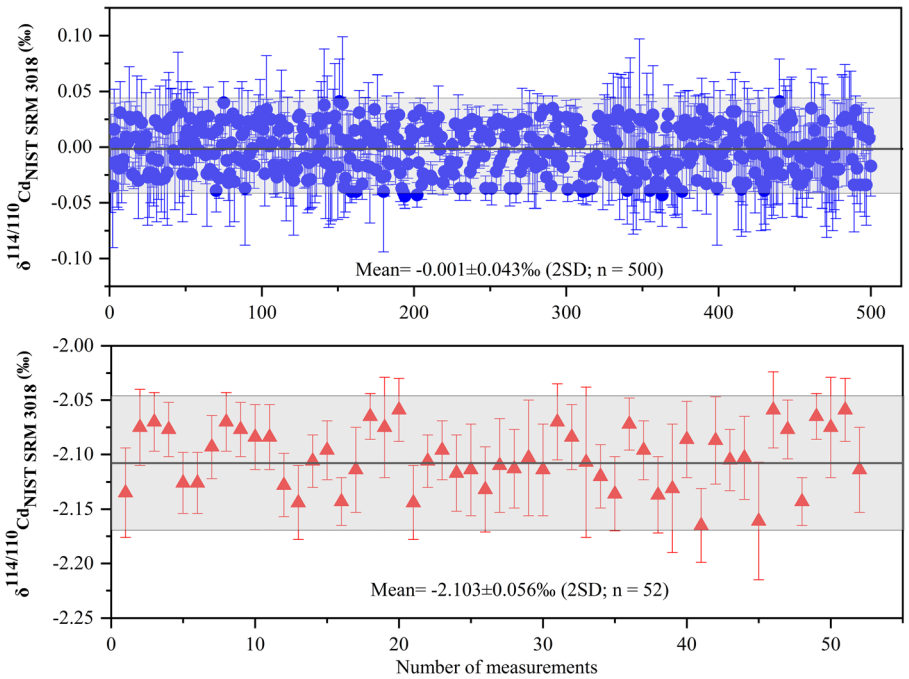

Fig. 3 The long-term reproducibility of the $\delta^{114/110}Cd_{NIST\ SRM\ 3018}$ values for (a) NIST SRM 3108 and (b) standard solution Spec-Cd. Error bars represent two standard errors of each measurement. The grey area represents twice the standard deviation of the $\delta^{114/110}Cd_{NIST\ SRM\ 3018}$ value of NIST SRM 3108 and Spec-Cd, respectively.

3.4. Procedural blanks

The total procedural blanks were determined by isotope dilution mass spectrometry. The total procedural blank from sample digestion to final Cd isotopic measurement is 0.042 ± 0.012 ng (2SD; $n = 6$), which is approximately 0.14% of the typical sample size (Cd = 30 ng) and negligible.

3.5. Cadmium isotopic compositions of geological and environmental reference materials

All the reference materials were independently digested and analysed ≥2 times utilising the proposed method to: (1) validate the accuracy of our proposed method; and (2) consolidate and enlarge the pre-existing database for international reference materials. The results are presented in Table 4 and Fig. 4, along with a compilation of published $\delta^{114/110}Cd_{NIST\ SRM\ 3018}$ values.

The measured $\delta^{114/110}Cd_{NIST\ SRM\ 3018}$ values of basalt BHVO-2, granodiorite GSP-2, shale SGR-1b, and carbonatite COQ-1 are in good agreement within uncertainty with published values (Table 4). BHVO-2 (0.048 ± 0.036‰) has a similar Cd isotopic composition to the upper continental crust (UCC; 0.03 ± 0.10)[63] and is slightly heavier than bulk silicate Earth (BSE; −0.06 ± 0.03).[63] GSP-2 (−0.191 ± 0.035‰) has a slightly lighter Cd isotopic composition relative to BSE and UCC, while for SGR-1b (0.076 ± 0.046‰) it approaches that of BSE and UCC. The shale standard materials SDO-1 and SCO-1 have been discontinued, and thus shale SGR-1b can be utilised as an alternative standard for shale samples. Dolomite GSR-12 has a $\delta^{114/110}Cd_{NIST\ SRM\ 3018}$ value of 0.162 ± 0.044‰ (2SD; $n = 9$), which is indistinguishable from the values for carbonatite COQ-1 (0.143 ± 0.053‰). Both GSR-12 and COQ-1 have slightly heavier Cd isotopic compositions relative to those of BSE and UCC.

The ferromanganese nodule NOD-P-1 has a $\delta^{114/110}Cd_{NIST\ SRM\ 3018}$ value of 0.185 ± 0.048‰ (2SD; $n = 9$), which is in agreement with published values (Table 4). The published $\delta^{114/110}Cd_{NIST\ SRM\ 3018}$ values of the ferromanganese nodule NOD-A-1 vary significantly from −0.16 ± 0.12‰ (ref. 58) to 0.23 ± 0.06‰.[64] Our measured value is 0.184 ± 0.057‰ (2SD; $n = 11$), which is in good agreement with most reported $\delta^{114/110}Cd_{NIST\ SRM\ 3018}$ values (Table 4). In addition to the variable Cd isotopic compositions, the Cd contents of NOD-A-1 (18.97 μg g^{-1}) determined by isotope dilution mass spectrometry in this study are also significantly different as compared with those reported in previous studies, such as 6.13 μg g^{-1} and 7.60 μg g^{-1} (Table 4). These results may suggest the heterogeneity of NOD-A-1.[50]

The measured $\delta^{114/110}Cd_{NIST\ SRM\ 3018}$ values of stream sediments GSD-3a and GSD-5a are consistent with their published values.[47,49] Data for stream sediment GSD-4a and soil GSS-1a are reported for the first time, and yielded $\delta^{114/110}$Cd values of 0.004 ± 0.047‰ (2SD; $n = 9$) and −0.078 ± 0.050‰ (2SD; $n = 8$), respectively. The Cd isotopic compositions of GSD-3a (−0.095 ± 0.055‰) and GSS-1a (−0.078 ± 0.050‰) are similar to those of BSE and UCC, while the Cd isotopic compositions of GSD-5a (0.062 ± 0.046‰) and GSD-4a approaches those of UCC and BSE. The mean $\delta^{114/110}Cd_{NIST\ SRM\ 3018}$ value of soil NIST 2711a is 0.568 ± 0.057‰ (2SD; $n = 7$), which is identical within uncertainty to the reported value for this standard (Table 4). NIST SRM 2711a was collected from Montana, USA, and has severe

Table 4 Cd isotopic composition of reference materials relative to NIST SRM 3108

Sample name	Sample type	Cd (μg g^{-1})	Reference	$\delta^{114/110}$Cd	2SD[d]	n[a]
Spex Cd	Reference solution		This study	−2.103	0.056	52
			Li *et al.* (2018)[59]	−2.130	0.090	
			Tan *et al.* (2020)[47]	−2.121	0.042	
			Zhong *et al.* (2023)[50]	−2.094	0.049	
BHVO-2	Basalt	0.088	This study	0.055	0.026	2
			This study	0.040	0.048	2
			Average (M = 2)[c]	**0.048**	**0.036**	**4**
			Liu *et al.*, (2019)[46]	0.039	0.047	
			Tan *et al.* (2020)[47]	−0.031	0.077	
			Lu *et al.* (2021)[66]	0.021	0.074	
			Zhong *et al.* (2023)[50]	−0.014	0.061	
			Chang *et al.* (2023)[51]	0.017	0.028	
GSP-2	Granodiorite	0.091	This study	−0.194	0.025	2
			This study	−0.188	0.053	2
			Average (M = 2)[c]	**−0.191**	**0.035**	**4**
			Liu *et al.* (2019)[46]	−0.196	0.068	
			Zhong *et al.* (2023)[50]	−0.228	0.079	
COQ-1	Carbonatite	0.611	This study	0.147	0.060	3
			This study	0.138	0.055	3
			Average (M = 2)[c]	**0.143**	**0.053**	**6**
			Liu *et al.* (2019)[46]	0.098	0.052	
			Zhong *et al.* (2023)[50]	0.123	0.048	
GSR-12	Dolomite	0.085	This study	0.153	0.057	3
			This study	0.181	0.018	3
			This study	0.154	0.031	3
			Average (M = 3)[c]	**0.162**	**0.044**	**9**
NOD-P-1	Manganese nodule	25.0	This study	0.185	0.048	3
			This study	0.180	0.055	3
			This study	0.181	0.052	3
			Average (M = 3)[c]	**0.185**	**0.048**	**9**
			Cloquet *et al.* (2005)[58,b]	0.03	0.12	
			Schmitt *et al.* (2009b)[65,b]	0.17	0.08	
			Horner *et al.* (2010)[64,b]	0.20	0.06[c]	
			Pallavicini *et al.* (2014)[44]	0.120	0.038	
			Li *et al.* (2018) (DS)[59]	0.21	0.03	
			Liu *et al.*, (2019)[46]	0.163	0.040	
			Tan *et al.* (2020)[50]	0.133	0.038	
			Peng *et al.* (2021)[49]	0.12	0.04	
			Borovička *et al.* (2021)[48]	0.14	0.07	
			Lu *et al.* (2021)[66]	0.135	0.074	
			Gou *et al.* (2022)[55]	0.16	0.04	
			Zhong *et al.* (2023)[50]	0.196	0.073	
NOD-A-1	Manganese nodule	20.8	This study	0.164	0.053	3
			This study	0.178	0.058	4
			This study	0.204	0.041	4
			Average (M = 3)[c]	**0.184**	**0.057**	**11**
			Cloquet *et al.* (2005)[58,b]	−0.17	0.12	
			Schmitt *et al.* (2009b)[65,b]	0.13	0.02	
			Horner *et al.* (2010)[64,b]	0.23	0.06[c]	
			Pallavicini *et al.* (2014)[44]	0.086	0.031	
			Murphy *et al.* (2016)[57]	0.17	0.05	
			Li *et al.* (2018)[59]	0.16	0.10	
			Tan *et al.* (2020)[47]	0.124	0.067	
			Peng *et al.* (2021)[49]	0.08	0.02	
			Zhong *et al.* (2023)[50]	0.193	0.047	
			Chang *et al.* (2023)[51]	0.133	0.038	
SGR-1b	Shale	1.21	This study	0.086	0.045	3
			This study	0.067	0.046	3
			Average (M = 2)[c]	**0.076**	**0.046**	**6**
			Tan *et al.* (2020)[47]	0.069	0.049	
			Lu *et al.* (2021)[66]	0.054	0.074	
GSD-3a	Stream sediment	0.519	This study	−0.081	0.043	3
			This study	−0.110	0.057	3
			Average (M = 2)[c]	**−0.095**	**0.055**	**6**
			Peng *et al.* (2021)[49]	−0.08	0.04	

Table 4 (*Contd.*)

Sample name	Sample type	Cd (μg g^{-1})	Reference	$\delta^{114/110}$Cd	2SD[d]	n[a]
GSD-4a	Stream sediment	1.05	This study	0.012	0.029	3
			This study	0.004	0.049	3
			This study	0.011	0.035	3
			Average (M = 3)[c]	**0.004**	**0.047**	**9**
GSD-5a	Stream sediment	1.52	This study	0.074	0.022	3
			This study	0.055	0.056	3
			Average (M = 3)[c]	**0.062**	**0.046**	**6**
			Tan *et al.* (2020)[47]	0.036	0.064	
			Peng *et al.* (2021)[49]	0.01	0.02	
NIST 2711a	Soil	54.1	This study	0.552	0.031	4
			This study	0.591	0.056	3
			Average (M = 2)[c]	**0.568**	**0.057**	**7**
			Li *et al.* (2018)[59]	0.57	0.07	
			Liu *et al.*, (2019)[46]	0.551	0.051	
			Tan *et al.* (2020)[47]	0.532	0.038	
			Borovička *et al.* (2021)[48]	0.57	0.05	
			Lu *et al.* (2021)[66]	0.561	0.055	
GSS-1a	Soil	2.98	This study	−0.073	0.055	3
			This study	−0.086	0.060	3
			This study	−0.072	0.050	2
			Average (M = 3)[c]	**−0.078**	**0.050**	**8**

[a] n – the number of measurements. [b] The $\delta^{114/110}$Cd value of samples in previous studies was recalculated relative to that of NIST SRM 3108, according to Abouchami *et al.* (2013).[67] [c] M – the number of independent digestions of the same reference material powder. [d] 2SD = 2 times the standard deviation of n repeated measurements.

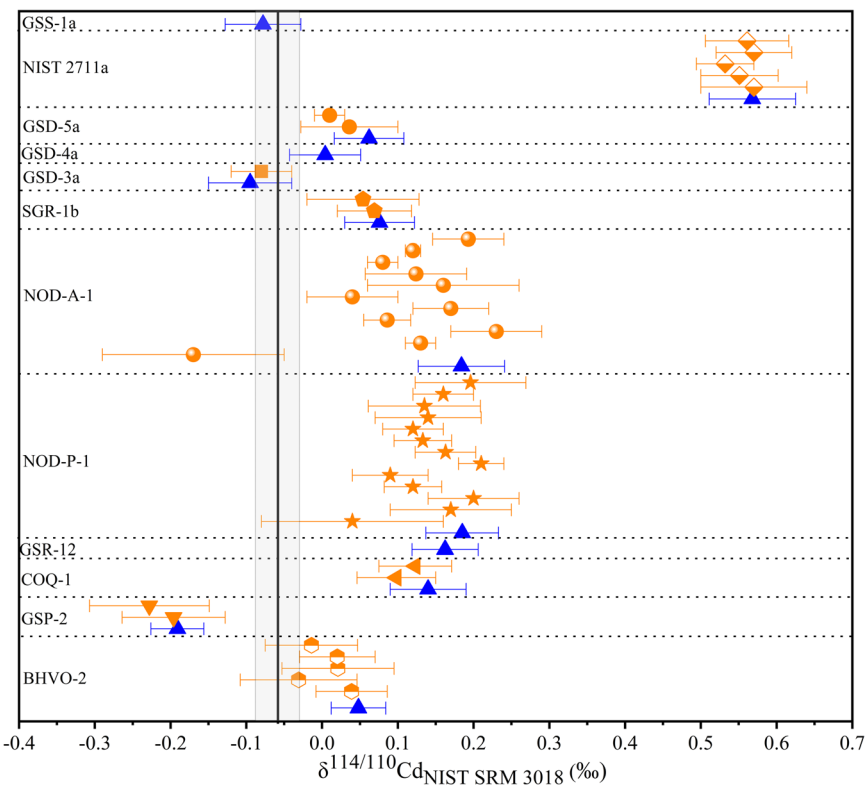

Fig. 4 $\delta^{114/110}Cd_{NIST\ SRM\ 3018}$ values of geological reference materials including the data from this study and previous studies. Blue triangle symbols represent the data from this study; other symbols represent the literature data (Table 4). Error bars reflect two standard deviations (2SD). The grey area represents the $\delta^{114/110}Cd_{NIST\ SRM\ 3018}$ value of Bulk Silicate Earth (−0.06 ± 0.03‰, 2SD).[63]

metal contamination with Cd contents of up to 54.1 μg g^{-1}. Furthermore, NIST SRM 2711a has a significantly positive $\delta^{114/110}Cd_{NIST\ SRM\ 3018}$ value relative to the BSE and UCC, and may have been contaminated by an anthropogenic source with a heavy Cd isotopic composition. This highlights the potential application of Cd isotopes for tracing sources of metal contamination.

4. Conclusions

We developed a new technique for separation of Cd from geological and environmental samples using a single-step AG-MP-1M (100–200 mesh) anion exchange resin column. The procedure takes advantage of the weak and strong affinity of Sn in 2 M HCl + 4 M HF and 0.005 M HCl + 2 M HF on AG-MP-1M anion exchange resin, respectively. Compared with previous methods, our technique is not only effective in reducing the matrix element/Cd ratios of all potentially interfering elements to negligible levels, but is also simple and efficient due to the single column separation step. As such, it is ideal for high-precision and accurate determination of Cd isotope ratios. The Cd isotopic compositions in geological and environmental reference materials determined with our method are in good agreement with published data, indicating that the proposed method is precise and accurate.

Conflicts of interest

There are no conflicts of interest to declare.

Acknowledgements

We are grateful to Prof. Zhu Jian-ming at the China University of Geosciences (Beijing) for providing the standard solution of Spex-Cd (Lot: CL8-71CDY). This work was financially supported by the Strategic Priority Research Program of the Chinese Academy of Sciences (Grant No. XDB42020201), the National Key Research and Development Project of China (grant number 2020YFA0714801) and National Science Foundation of China (grant number 41703001). The partial experiments of determining the Cd separation procedure were conducted in Tongwei Analytical Technology Co., Ltd (Guiyang), and therefore, we would like to acknowledge the help from Tongwei Analytical Technology Co., Ltd (Guiyang). This is contribution No. IS-3400 from GIGCAS.

References

1 W. F. McDonough and S. Sun, *Chem. Geol.*, 1995, **120**, 223–253.
2 F. Wombacher, M. Rehkämper, K. Mezger and C. Münker, *Geochim. Cosmochim. Acta*, 2003, **67**, 4639–4654.
3 W. Pritzkow, S. Wunderli, J. Vogl and G. Fortunato, *Int. J. Mass Spectrom.*, 2007, **261**, 74–85.
4 F. Lacan, R. Francois, Y. Ji and R. M. Sherrell, *Geochim. Cosmochim. Acta*, 2006, **70**, 5104–5118.
5 R. Wei, Q. Guo, H. Wen, C. Liu, J. Yang, M. Peters, J. Hu, G. Zhu, H. Zhang, L. Tian, X. Han, J. Ma, C. Zhu and Y. Wan, *Sci. Rep.*, 2016, **6**, 24309.
6 M. Wiggenhauser, M. Bigalke, M. Imseng, M. Muller, A. Keller, K. Murphy, K. Kreissig, M. Rehkämper, W. Wilcke and E. Frossard, *Environ. Sci. Technol.*, 2016, **50**, 9223–9231.
7 T. J. Horner, R. E. M. Rickaby and G. M. Henderson, *Earth Planet. Sci. Lett.*, 2011, **312**, 243–253.
8 L. E. Wasylenki, J. W. Swihart and S. J. Romaniello, *Geochim. Cosmochim. Acta*, 2014, **140**, 212–226.
9 D. Guinoiseau, S. J. G. Galer and W. Abouchami, *Earth Planet. Sci. Lett.*, 2018, **498**, 300–308.
10 X. Xie, L. Yan, J. Li, L. Guan and Z. Chi, *Sci. Total Environ.*, 2020, **760**, 143330.
11 X. Yan, M. Zhu, W. Li, C. L. Peacock, J. Ma, H. Wen, F. Liu, Z. Zhou, C. Zhu and H. Yin, *Environ. Sci. Technol.*, 2021, **55**, 11601–11611.
12 H. Peng, P. Liu, H. Zheng, N. S. Belshaw and S. Hu, *Chem. Geol.*, 2023, **622**, 121341.
13 Y. Zhang, H. Wen, C. Zhu, H. Fan, C. Luo, J. Liu and C. Cloquet, *Environ. Pollut.*, 2016, **216**, 9–17.
14 M. Imseng, M. Wiggenhauser, A. Keller, M. Muller, M. Rehkämper, K. Murphy, K. Kreissig, E. Frossard, W. Wilcke and M. Bigalke, *Environ. Sci. Technol.*, 2018, **52**, 1919–1928.
15 C. Zhu, H. Wen, Y. Zhang, R. Yin and C. Cloquet, *Sci. Total Environ.*, 2018, **616–617**, 64–72.
16 C. Cloquet, J. Carignan, G. Libourel, T. Sterckeman and E. Perdrix, *Environ. Sci. Technol.*, 2006, **40**, 2525–2530.
17 A. E. Shiel, D. Weis and K. J. Orians, *Sci. Total Environ.*, 2010, **408**, 2357–2368.
18 E. Martinková, V. Chrastný, M. Francová, A. Šípková, J. Čuřík and O. Myška, *J. Hazard. Mater.*, 2016, **302**, 114–119.
19 F. Fouskas, L. Ma, M. A. Engle, L. Ruppert, N. J. Geboy and M. A. Costa, *Appl. Geochem.*, 2018, **96**, 100–112.
20 Q. Zhong, M. Yin, Q. Zhang, J. Beiyuan, Z. Zhang, J. Liu, X. Yang, J. Wang, L. Wang, Y. Jiang, T. Xiao and Z. Zhang, *J. Hazard. Mater.*, 2021, **411**, 125015.
21 F. Wombacher, M. Rehkämper, K. Mezger, A. Bischoff and C. Münker, *Geochim. Cosmochim. Acta*, 2008, **72**, 646–667.
22 B. Gao, H. Zhou, X. Liang and X. Tu, *Environ. Pollut.*, 2013, **181**, 340–343.
23 C. Zhu, H. Wen, Y. Zhang, H. Fan, S. Fu, J. Xu and T. Qin, *Sci. China: Earth Sci.*, 2013, **56**, 2056–2065.
24 W. Abouchami, S. J. G. Galer, H. J. W. de Baar, R. Middag, D. Vance, Y. Zhao, M. Klunder, K. Mezger, H. Feldmann and M. O. Andreae, *Geochim. Cosmochim. Acta*, 2014, **127**, 348–367.
25 T. M. Conway and S. G. John, *Geochim. Cosmochim. Acta*, 2015, **148**, 269–283.
26 H. Wen, Y. Zhang, C. Cloquet, C. Zhu, H. Fan and C. Luo, *Appl. Geochem.*, 2015, **52**, 147–154.
27 D. J. Janssen, W. Abouchami, S. J. G. Galer and J. T. Cullen, *Earth Planet. Sci. Lett.*, 2017, **472**, 241–252.

28 M. Salmanzadeh, A. Hartland, C. H. Stirling, M. R. Balks, L. A. Schipper, C. Joshi and E. George, *Environ. Sci. Technol.*, 2017, **51**, 7369–7377.
29 E. George, C. H. Stirling, M. Gault-Ringold, M. J. Ellwood and R. Middag, *Earth Planet. Sci. Lett.*, 2019, **514**, 84–95.
30 M. Sieber, T. M. Conway, G. F. D. Souza, H. Obata and D. Vance, *Chem. Geol.*, 2018, **511**, 494–509.
31 P. Wang, Z. Li, J. Liu, X. Y. Bi, Y. Q. Ning, S. C. Yang and X. J. Yang, *Environ. Pollut.*, 2019, **249**, 208–216.
32 J. A. Frederiksen, R. M. Klaebe, J. Farka, P. K. Swart and R. Frei, *Sci. Total Environ.*, 2022, **806**, 150565.
33 X. Zhang, Y. Yan, S. A. Wadood, Q. Sun and B. Guo, *Appl. Geochem.*, 2020, 123.
34 Q. H. Zhong, Y. C. Zhou, D. C. W. Tsang, J. Liu, X. Yang, M. L. Yin, S. J. Wu, J. Wang, T. F. Xiao and Z. F. Zhang, *Sci. Total Environ.*, 2020, **736**, 139585.
35 A. L. Bryan, A. J. Dickson, F. Dowdall, W. B. Homoky, D. Porcelli and G. M. Henderson, *Earth Planet. Sci. Lett.*, 2021, **565**, 116946.
36 R. Frei, L. Xu, J. A. Frederiksen and B. Lehmann, *Chem. Geol.*, 2021, 563.
37 T. Wu, Z. Huang, Y. He, M. Yang, H. Fan, C. Wei, L. Ye, Y. Hu, Z. Xiang and C. Lai, *Ore Geol. Rev.*, 2021, 135.
38 D. J. Janssen, W. Abouchami, S. J. G. Galer, K. B. Purdon and J. T. Cullen, *Earth Planet. Sci. Lett.*, 2019, **515**, 67–78.
39 K. J. R. Rosman and J. R. De Laeter, *Nature*, 1976, **261**, 216–218.
40 K. J. R. Rosman and J. R. De Laeter, *Earth Planet. Sci. Lett.*, 1988, **89**, 163–169.
41 S. Ripperger and M. Rehkämper, *Geochim. Cosmochim. Acta*, 2007, **71**, 631–642.
42 A. D. Schmitt, S. J. G. Galer and W. Abouchami, *J. Anal. At. Spectrom.*, 2009, **24**, 1079–1088.
43 Z. Xue, M. Rehkämper, M. Schonbachler, P. J. Statham and B. J. Cole, *Anal. Bioanal. Chem.*, 2012, **402**, 883–893.
44 N. Pallavicini, E. Engstrom, D. C. Baxter, B. Ohlander, J. Ingri and I. Rodushkin, *J. Anal. At. Spectrom.*, 2014, **29**, 1570–1584.
45 R. Wei, Q. Guo, H. Wen, J. Yang, M. Peters, C. Zhu, J. Ma, G. Zhu, H. Zhang and L. Tian, *Anal. Methods*, 2015, **7**, 2479–2487.
46 M. S. Liu, Q. Zhang, Y. Zhang, Z. Zhao, F. Huang and H. M. Yu, *Geostand. Geoanal. Res.*, 2019, **44**, 169–182.
47 D. Tan, J.-M. Zhu, X. Wang, G. Han, Z. Lu and W. Xu, *J. Anal. At. Spectrom.*, 2020, **35**, 713–727.
48 J. Borovicka, L. Ackerman and J. Rejsek, *Talanta*, 2021, **221**, 121389.
49 H. Peng, D. He, R. Guo, X. Liu, N. S. Belshaw, H. Zheng, S. Hu and Z. Zhu, *J. Anal. At. Spectrom.*, 2021, **36**, 390–398.
50 Q. H. Zhong, J. Li, L. Yin, N. P. Shen, S. Yan, Z. Y. Wang and C. H. Zhu, *J. Anal. At. Spectrom.*, 2023, **38**, 939.
51 H. Chang, J. M. Zhu, X. L. Wang and T. Gao, *J. Anal. At. Spectrom.*, 2023, **38**, 950–962.
52 Z. Lu, J. M. Zhu, D. Tan, T. M. Johnson and X. L. Wang, *Anal. Chem.*, 2021, **95**, 2253–2259.
53 S. V. Hohl, S. Y. Jiang, H. Z. Wei, D. H. Pi, Q. Liu, S. Viehmann and S. J. G. Galer, *Geochim. Cosmochim. Acta*, 2019, **263**, 1–20.
54 T. C. Sweere, A. J. Dickson, H. C. Jenkyns, D. Porcelli, M. Ruhl, M. J. Murphy, E. Idiz, B. S. H. J. M. van den, H. J. M. Sander, J. S. Eldrett and G. M. Henderson, *Geochim. Cosmochim. Acta*, 2020, **287**, 251–262.
55 C. Guo, T. Li, G. Li, T. Chen, L. Li, L. Zhao and J. Ji, *J. Anal. At. Spectrom.*, 2022, **37**, 2470–2479.
56 M. Gault-Ringold and C. H. Stirling, *J. Anal. At. Spectrom.*, 2012, **27**, 449.
57 K. Murphy, M. Rehkamper, K. Kreissig, B. Coles and T. van de Flierdt, *J. Anal. At. Spectrom.*, 2016, **31**, 319–327.
58 C. Cloquet, O. Rouxel, J. Carignan and G. Libourel, *Geostand. Geoanal. Res.*, 2005, **29**, 95–106.
59 D. Li, M. L. Li, W. R. Liu, Z. Z. Qin and S. A. Liu, *Geostand. Geoanal. Res.*, 2018, **42**, 593–605.
60 L. Zhang, Z. Y. Ren, X. P. Xia, J. Li and Z. F. Zhang, *Int. J. Mass Spectrom.*, 2015, **392**, 118–124.
61 R. D. Loss, K. J. R. Rosman and J. R. De Laeter, *Geochim. Cosmochim. Acta*, 1990, **54**, 3525–3536.
62 N. Braukmüller, F. Wombacher, A. Bragagni and C. Münker, *Geostand. Geoanal. Res.*, 2020, **44**, 733–752.
63 H. Pickard, E. Palk, M. Schonbachler, R. E. T. Moore, B. J. Coles, K. Kreissig, K. Nilsson-KerR, S. J. Hammond, E. Takazawa, C. Hemond, P. Tropper, D. N. Barfod and M. Rehkamper, *Geochim. Cosmochim. Acta*, 2022, **338**, 165–180.
64 T. J. Horner, M. Schönbächler, M. Rehkämper, S. G. Nielsen, H. Williams, A. N. Halliday, Z. Xue and J. R. Hein, *Geochem., Geophys., Geosyst.*, 2010, 1–10.
65 A.-D. Schmitt, S. J. G. Galer and W. Abouchami, *Earth Planet. Sci. Lett.*, 2009, **277**, 262–272.
66 Z. Lu, J. M. Zhu, D. Tan, X. Wang and Z. Zheng, *Geostand. Geoanal. Res.*, 2021, **45**, 565–581.
67 W. Abouchami, S. J. G. Galer, T. J. Horner, M. Rehkämper, F. Wombacher, Z. Xue, M. Lambelet, M. Gault-Ringold, C. H. Stirling and M. Schonbachler, *Geostand. Geoanal. Res.*, 2013, **37**, 5–17.